Role of baryons in chiral-symmetry restoration at high temperature

Carleton DeTar
Department of Physics, University of Utah, Salt Lake City, Utah 84112
(Received 26 February 1990)

To help provide insight into the apparent remarkable rise in baryon susceptibility at the high-temperature phase transition in QCD, we study the three-dimensional lattice SU(2) chiral model at finite temperature. The purpose of this study is to determine the extent to which a rising susceptibility is a natural consequence of chiral-symmetry restoration in a nonlinear σ model. Indeed the susceptibility, defined in terms of a discrete (nonconserved) version of the winding number, is found to rise rapidly in the vicinity of the phase transition, suggesting that a proliferation of baryons and antibaryons (i.e., Skyrmions) plays a significant role in the restoration of the chiral symmetry. These results support the idea that the cooling of the quark plasma could result in copious antibaryon production.

I. INTRODUCTION

Numerical simulations of QCD with quarks suggest that the baryon susceptibility, defined in the usual way in terms of the quark baryon number, rises dramatically at the high-temperature phase transition in a manner suggestive of the liberation of light baryonic degrees of freedom[1] (i.e., quarks). Paradoxically, similar simulations provide no evidence for such light degrees of freedom in measurements of the high-temperature static screening lengths.[2] Indeed, current evidence suggests that long-range screening in the quark plasma is controlled by hadronic modes, the longest range of which are most likely high-temperature pionlike and σ-like modes, which are degenerate in the chiral limit. Screening in the baryon channel is governed by rather short-range high-temperature parity-doubled analogs of the nucleon. Thus it is important to seek other explanations of the rise in the baryon susceptibility. In this paper we suggest that the phenomenon is a natural consequence of the restoration of chiral symmetry and is brought about by a proliferation of field configurations with baryonic topology.

A classic example of symmetry restoration at finite temperature is provided by the $\lambda\phi^4$ theory with a symmetry-breaking potential $V(\phi)$. The traditional analysis of symmetry restoration is based on perturbation theory.[3] From this point of view the phase transition occurs because the entropy as a function of the mean field $S(\bar{\phi})$ of the nearly free gas of mesons has a maximum at zero mean field. Thus the mean-field free energy $F(\bar{\phi}) = E(\bar{\phi}) - TS(\bar{\phi})$ is minimum at $\bar{\phi} = 0$ for sufficiently high temperature T. At strong coupling, however, the perturbative analysis breaks down qualitatively, since other mechanisms for disorder predominate. In particular, the formation of domain walls or solitons becomes energetically favorable at strong coupling. Such structures must be treated by nonperturbative methods.

There is strong evidence from numerical simulation[2,4] that the finite-temperature phase transition in QCD restores the SU(N)×SU(N)×U(1) chiral symmetry. The temperature of the phase transition is estimated to be roughly in the range 100–200 MeV.[5] Since numerical simulations also give evidence for the presence of confined hadronic modes in the high-temperature phase, at least close to the phase transition, we believe it is plausible to model the phase transition in terms of a chiral field theory in which the elementary degrees of freedom are π mesons, both at low and high temperature. This model is offered as a rough description of the long-range behavior of QCD, both below and above the phase transition. The model is intended to provide insight into the mechanism of chiral-symmetry restoration in QCD. Insights gained from such a model suggest interesting tests for simulations based upon full QCD.

Although the σ meson has never been firmly established, as a representation of the $\pi\pi$ S-wave enhancement, it must have a mass of several hundred MeV. It is apparent that a linear σ model for the π and σ mesons must be strongly coupled in order to produce such a large mass. Since the σ mass is much larger than the pion mass, the pion decay constant f_π, and the temperature of the phase transition T_c, it is plausible that strong coupling is required at temperatures close to the phase transition as well. Therefore a phenomenology of chiral-symmetry restoration based solely on perturbation theory, although perhaps tempting,[6] is implausible. For these reasons we choose to investigate the SU(2)×SU(2) or O(4) nonlinear chiral model at finite temperature. The fundamental field is a four-vector $U(x)$ on the unit three-sphere S^3.

At high temperature the lattice-Feynman-path integral may be reduced to three dimensions. On each site **r** of a

three-dimensional periodic lattice, we introduce an O(4) field in the form of an SU(2) matrix

$$U(\mathbf{r}) = u_4 + i\sigma \cdot \mathbf{u} \tag{1}$$

with Pauli matrices σ and $|u|^2 = 1$. The Hamiltonian is then

$$H/E_0 = \sum_{(\mathbf{rs})} \{1 - \tfrac{1}{2} \operatorname{Tr}[U(\mathbf{r})U^\dagger(\mathbf{s})]\} + \beta_3 \sum_{\mathbf{r}} [1 - \tfrac{1}{2} \operatorname{Tr} U(\mathbf{r})], \tag{2}$$

where E_0 sets the energy scale. Here the notation (rs) refers to unique nearest-neighbor pairs. A symmetry-breaking term has been included. For lattice constant $a \to 0$ the Hamiltonian has the naive continuum limit

$$Ha/E_0 = \tfrac{1}{4} \int d\mathbf{r} \operatorname{Tr} |\partial_\mu U|^2 + \beta_3 a^{-2} \int d\mathbf{r} (1 - \tfrac{1}{2} \operatorname{Tr} U). \tag{3}$$

Comparing this expression with the conventional continuum limit,

$$H = \frac{F_\pi^2}{16} \int d\mathbf{r} \operatorname{Tr} |\partial_\mu U|^2 + \frac{F_\pi^2 m_\pi^2}{4} \int d\mathbf{r} (1 - \tfrac{1}{2} \operatorname{Tr} U), \tag{4}$$

suggests the identification

$$E_0/a = F_\pi^2/4 \ , \quad \beta_3 = F_\pi^2 m_\pi^2 a^3/4E_0. \tag{5}$$

The high-temperature partition function is given by

$$Z = \int \prod [dU(\mathbf{r})] \exp(-\beta_1 H), \tag{6}$$

where the temperature is given by

$$T = E_0/\beta_1. \tag{7}$$

Without a Skyrme term the continuum-nonlinear-chiral model does not have a stable baryon (Skyrmion) at zero temperature. Likewise, we have not encountered stable baryonic configurations in the lattice version of the model. If such stability were required, the obvious next step would be to include a lattice version of the Skyrme term.[7,8] That is the goal of the second part of this study, discussed in Secs. IV and V.

Is Skyrmion stability important for a finite-temperature study? Stability offers advantages and disadvantages. Thermal excitations with nonzero winding number occur whether or not stable zero-temperature structures exist. If these configurations do not persist indefinitely in the simulation, it is possible to simulate the grand-canonical ensemble in baryon number. However, stability at low temperature is desirable in a more completely realistic theory. A stable low-temperature structure can be compared with a known hadron, making it possible to assign physical values to the parameters of the model. One may also want to look for a connection between the spatial fluctuations in baryon number of the high-temperature configurations and the spatial distribution of baryon number in the low-temperature structures. However, in the absence of Skyrmion stability, one may still hope for a qualitative understanding of the topological features of the phase transition. That is the goal of the first part of this study, discussed in Secs. II and III.

The remainder of the paper is organized as follows. In Sec. II we discuss our discrete definition of the winding number (baryon number). In Sec. III we present results of the simulation with the basic Hamiltonian (2). We find a large rise in the baryon susceptibility in the vicinity of the phase transition. To compare this rise with the QCD result requires a matching of lattice scales. However, without stable zero-temperature Skyrmions, there is no obvious way to attempt a numerical comparison. To make further progress we discuss the introduction of a Skyrme-stabilization term, in Sec. IV. With a suitable choice of the weight for this term large, classically stable Skyrmion configurations (radius several lattice units or more) such as the continuum Skyrmions can be obtained. However, they are not robust with our choice of lattice Hamiltonian. That is, at low, but finite temperature, such large Skyrmions are rarely found, presumably because they are not sufficiently stable. Fortunately, at other choices of the weight of the stabilization term, small Skyrmions (a couple of lattice units) can be made to live sufficiently long to permit a rough estimate of their size and energy. To further elucidate the mechanical properties of the phase transition, lattice configurations were subjected to a cooling treatment, with results described in Sec. V. Finally, possible consequences for QCD and for searches for quark matter are discussed in Sec. VI.

II. WINDING NUMBER ON THE LATTICE

For a continuous map $U(x)$ of S^3 into S^3, the baryon number density is defined by

$$\rho_B = \frac{1}{24\pi^2} \operatorname{Tr} \mathbf{A} \cdot \mathbf{A} \times \mathbf{A}, \tag{8}$$

where $\mathbf{A} = U\nabla U$.[9] The winding number is the integral of this quantity over the spatial volume V. We equate this number with the baryon number. Whether a soliton with *winding* number B should be counted as having *baryon* number B can be answered only after fermions are included explicitly in the model. Studies of small Skyrmions interacting with fermions have shown that the integer baryon number can be regarded as being shared between the soliton and the fermion, with the soliton's share decreasing with soliton size.[10] Since the winding number counts "small" and "large" solitons alike, and we have not included fermions, our model is incomplete. Therefore, we are assuming that the susceptibility defined through the winding number gives a good approximation to the baryon susceptibility that would be found in a theory with fermions present.

Suppose that the region V in coordinate space R^3 is mapped to the region $B \in S^3$. Then the total baryon number in V is just the oriented volume of B, with the

convention that the total volume of S^3 is 1. An infinitesimal tetrahedron $dV \subset R^3$ maps approximately into an infinitesimal tetrahedron $dB = U(dV) \subset S^3$. If dV is an infinitesimal tetrahedron with vertices a, b, c, d, which map, respectively, to u_a, u_b, u_c, u_d, then the oriented volume dB is approximately

$$\rho(dB) = \frac{1}{12\pi^2}\epsilon_{\mu\lambda\rho\sigma}u_a^\mu u_b^\lambda u_c^\rho u_d^\sigma. \tag{9}$$

On a lattice of finite spacing, a crude estimate of the total baryon number can be obtained by dissecting the lattice into elementary tetrahedra dV and forming the sum of these approximants. Each unit cube in the lattice can be dissected into five such tetrahedra. A possible improvement on this approximant would bound the facets of the image tetrahedra $dB = U(dV)$ by sections of great spheres in S^3 so that contiguous volumes dV would map onto contiguous volumes $dB = U(dV)$. In fact, rather cumbersome exact integral expressions do exist for the volume of such a bounded region. However, if only the global winding number of the entire map is desired, then there is a much more elegant procedure: count the number of times the map crosses a particular point u_p (say, the north pole) of S^3. Count plus one for a positive crossing and minus one for a negative crossing (defined below). The global winding number is then the algebraic sum of these values. Specifically, we define the global winding number

$$B = \sum_{dV \in V} q_{U(dV)}, \tag{10}$$

where

$$q_{dB} = \begin{cases} +1 & \text{if } u_p \in dB \text{ and } \rho(dB) > 0, \\ -1 & \text{if } u_p \in dB \text{ and } \rho(db) < 0, \\ 0 & \text{if } u_p \notin dB. \end{cases} \tag{11}$$

Deciding whether u_p is in dB involves an arbitrary choice because of the discreteness of the lattice. A natural procedure is to make a smooth interpolation between the vertices u_a, u_b, u_c, u_d of dB. Then if u_p is found in the region bounded by the interpolation, we say that $u_p \in dB$. Mathematically, our test for inclusion involves constructing four new tetrahedra from the vertices u_a, u_b, u_c, u_d by replacing the vertices one by one with u_p. Thus we form $dB_a = \{u_p, u_b, u_c, u_d\}$, $dB_b = \{u_a, u_p, u_c, u_d\}$, etc. Then u_p is in dB if all of the volumes $\rho(dB_a)$, $\rho(dB_b)$, etc., have the same sign as $\rho(dB)$.

An ambiguity arises if any of the five volumes is zero. Although mathematically such an occurrence is a set of measure zero, numerically, all too frequently in lattices of the size used in this study, the volume measurement is zero within the precision of 32-bit arithmetic. Thus there is a potential for a miscalculation of the winding number resulting from round-off errors. However, with care this error can be rigorously avoided. The necessary precautions involve arranging a systematic dissection of the lattice cubes into tetrahedra so that adjacent cubes share the same triangular facets, and arranging so that any round-off error is treated consistently between tetrahedra with shared facets. In this way there are no gaps in the map U and round-off errors introduce no inessential ambiguities in the determination of the global lattice winding number.

III. FINITE-TEMPERATURE PHASE TRANSITION

The first goal of the simulation is to locate the finite-temperature phase transition. The SU(2) chiral model with $\beta_3 = 0$ has been studied extensively by Kogut and co-workers,[11] and it is well known that the chiral-symmetry-restoring phase transition is continuous. The phase transition can be located by studying the behavior of the order parameter $\sigma = \mathrm{Tr}\, U/2$ as a function of the coupling β_1. It can also be located by studying the screening mass associated with the Goldstone boson. This screening mass is defined from the correlation

$$S_\pi(z) = \langle \bar{\mathbf{U}}(0) \cdot \bar{\mathbf{U}}(z) \rangle, \tag{12}$$

where $\mathbf{U}$ denotes the three-vector component of U and $\bar{U}(z)$ signifies averaging over a plane perpendicular to the z axis at z. The screening mass is given by the asymptotic form of this correlation:

$$S_\pi(z) \approx a + b\exp(-\mu_\pi z). \tag{13}$$

Similarly, one may define the screening mass μ_σ for the σ meson channel through the correlation

$$S_\sigma(z) = \langle \mathrm{Tr}\, \bar{U}(0)\, \mathrm{Tr}\, \bar{U}(z) \rangle. \tag{14}$$

Neither of these correlations is chirally invariant, so it is necessary to define them by first introducing an explicit symmetry-breaking term [i.e., the term in β_3 in Eq. (2)], second, taking the infinite-volume limit, and finally, taking the limit of vanishing β_3. In practice this limit is estimated by the less rigorous method of extrapolating the finite-volume calculation to zero β_3.

Shown in Fig. 1 is σ vs β_1 for four values of the symmetry-breaking parameter β_3. The extrapolation of σ to the chiral limit is shown in Fig. 2 for a few temperatures. In mean-field theory, it is expected that the order parameter vanishes as β_3 in the symmetry restored phase and $\beta_3^{1/3}$ precisely at the phase transition. From these results, it is plausible that the order parameter vanishes in the chiral limit at inverse temperatures $\beta_1 = 0.80$ and 0.90, and give a nonzero intercept at 0.95 and 1.00. Thus the phase transition occurs in the region 0.90–0.95.

As a further check, we consider correlation lengths. The pion screening mass is shown as a function of β_1 in Fig. 3 for various values of the symmetry-breaking parameter, and in Fig. 4 for two values of the inverse temperature near the phase transition. The extrapolation to the chiral limit appears to be consistent with zero at $\beta_1 = 0.95$ and not zero at $\beta_1 = 0.90$, in agreement with the results for the order parameter. Our value on a 30^3 lattice is to be compared with the estimate 0.81 for a 9^3 lattice.[11]

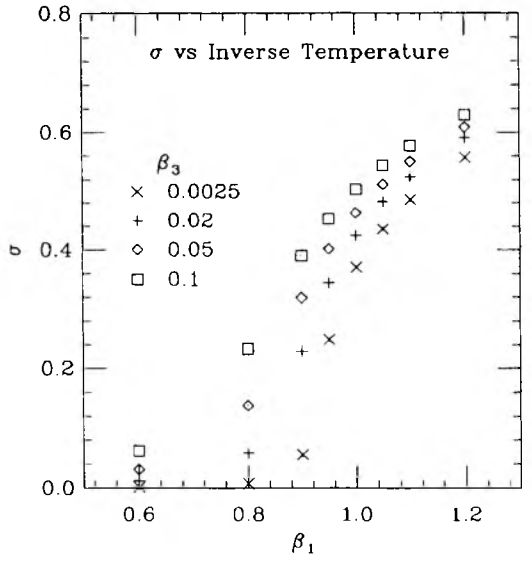

FIG. 1. The order parameter σ vs inverse temperature for four values of the symmetry-breaking parameter β_3. Statistical errors are smaller than the plot symbols.

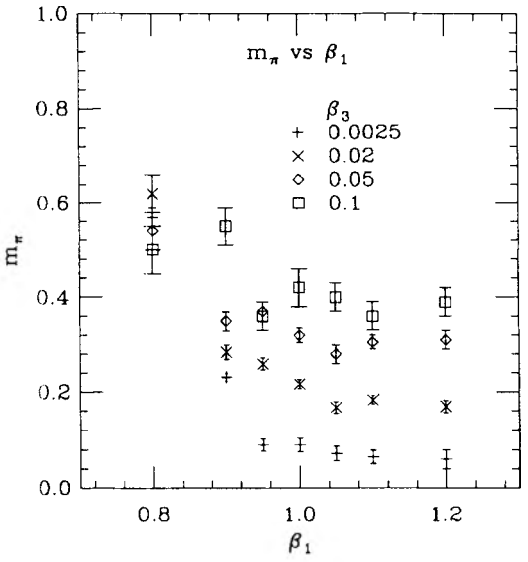

FIG. 3. Pion screening mass vs inverse temperature for four values of the symmetry-breaking parameter β_3.

Shown in Table I are screening masses for both the π and σ as a function of inverse temperature and symmetry-breaking parameter. It is plausible from these results that for $\beta_1 > 0.95$ the pion and σ screening masses are equal within errors in the chiral limit as expected from a restoration of the SU(2)×SU(2) symmetry, and they are not equal for $\beta_1 \leq 0.95$. At low temperature the σ meson mass is less well determined from the correlation function. Fits to the correlation function starting at zero separation give a much higher screening mass than fits starting one or two lattice units away. This behavior may reflect the effects of the two-pion continuum. The screening masses quoted in the table are taken from fits starting at a separation of one or two lattice sites, and so represent the lower mass portion of the spectrum.

We now turn to the susceptibility. Shown in Fig. 5 is the variance of the total baryon number $\langle B^2 \rangle$ as a function of inverse temperature β_1. This quantity is related to the susceptibility through

$$\chi_B = (\langle B^2 \rangle - \langle B \rangle^2)/VT, \tag{15}$$

where V is the volume of the lattice and T is the temperature. Since we are working in the grand-canonical

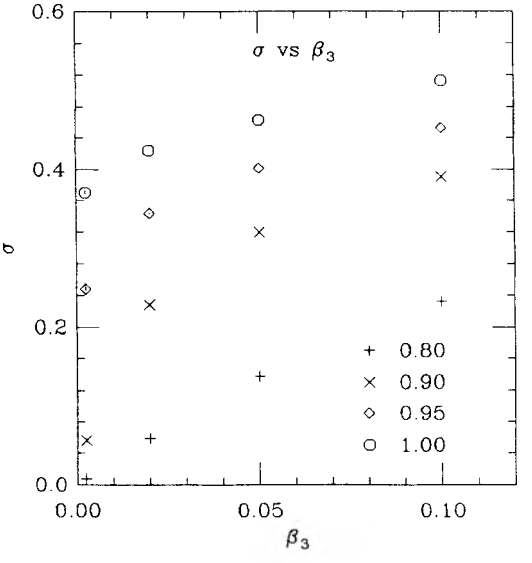

FIG. 2. The order parameter σ vs the symmetry-breaking parameter for four values of the inverse temperature.

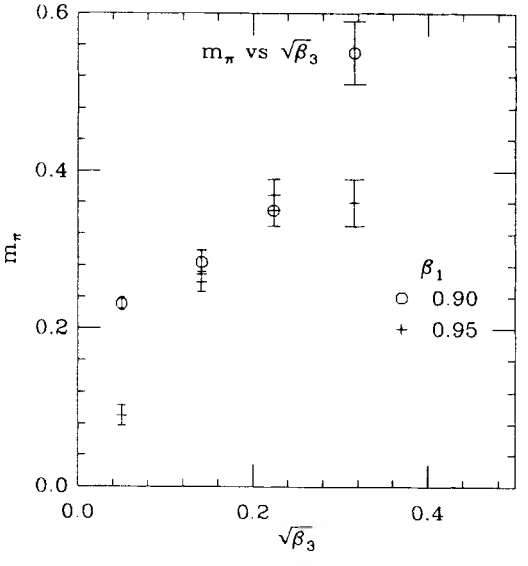

FIG. 4. Pion screening mass vs the symmetry-breaking parameter for two values of the inverse temperature near the phase transition.

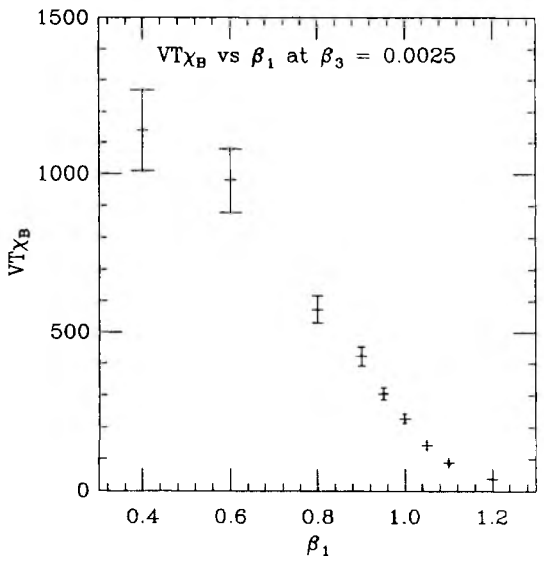

FIG. 5. Susceptibility vs inverse temperature for a small value of the symmetry-breaking parameter.

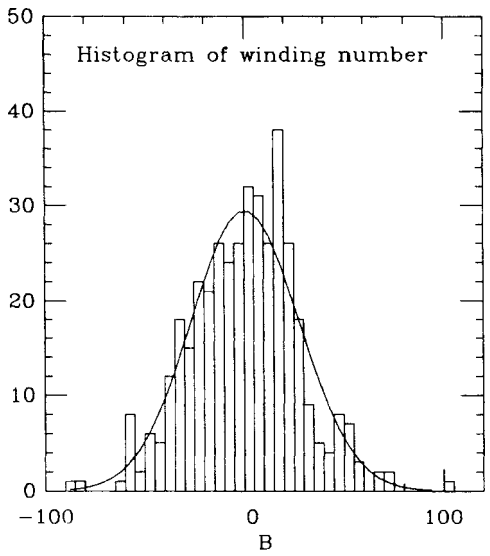

FIG. 6. Histogram of the total winding number B for a 30^3 lattice at $\beta_1 = 0.8$ and $\beta_3 = 0.0025$. The curve plots a normal distribution with a variance set equal to the observed value $\langle B^2 \rangle$.

ensemble at zero chemical potential, the mean baryon number vanishes: $\langle B \rangle = 0$. We see that at low temperature the susceptibility is relatively small, and there is a rapid rise in the vicinity of the phase transition. The susceptibility continues to rise in the high-temperature phase.

To explore this result further, we examine the distribution in baryon number for the simulation at $\beta_1 = 0.8$ and $\beta_3 = 0.0025$. Shown in Fig. 6 is the histogram for a 30^3 lattice and in Fig. 7 for a 20^3 lattice. These histograms agree rather well with a random-walk formula

$$P = \frac{1}{\sqrt{2\pi\chi_B VT}} \exp[-B^2/(2\chi_B VT)], \tag{16}$$

also plotted in the figure. (The three points around winding number 100 and -100 on the 30^3 lattice are exceptions to this statement.) Thus the susceptibility is not only an intensive quantity, as expected, but there is also little evident interaction correlating clusters of baryons. Thus $1/(2\chi_B T)$ gives a measure of the average volume in which a random fluctuation contributes $+1$ or -1 to the total winding number translated into a spherical region; this size corresponds to a sphere of radius determined by

$$r_{\text{eff}}^3 = 3V/\left(8\pi\langle B^2\rangle\right). \tag{17}$$

That is r_{eff} is in the range $2a$ to $3a$ in lattice units in the vicinity of the phase transition.

TABLE I. Pion and σ screening masses in the SU(2)×SU(2) chiral model with symmetry-breaking parameter β_3 as a function of inverse temperature β_1.

		β_3			
β_1		0.0025	0.02	0.05	0.1
0.60	m_π	0.92(13)	1.6(4)	0.85(13)	1.1(2)
0.60	m_σ	1.34(4)	1.18(4)	1.28(4)	1.16(4)
0.80	m_π	0.57(2)	0.62(4)	0.54(4)	0.50(5)
0.80	m_σ	0.574(15)	0.49(4)	0.64(2)	0.76(3)
0.90	m_π	0.231(8)	0.284(15)	0.35(2)	0.55(4)
0.90	m_σ	0.209(15)	0.44(2)	0.49(6)	0.5(2)
0.95	m_π	0.090(13)	0.259(13)	0.37(2)	0.36(3)
0.95	m_σ	0.26(2)	0.55(2)	0.77(2)	0.61(14)
1.00	m_π	0.090(14)	0.216(10)	0.320(15)	0.42(4)
1.00	m_σ	0.34(3)	0.66(2)	0.55(7)	0.96(5)
1.05	m_π	0.072(15)	0.158(13)	0.28(2)	0.40(3)
1.05	m_σ	0.20(5)	0.59(9)	0.59(7)	0.75(15)
1.10	m_π	0.064(14)	0.183(9)	0.305(15)	0.36(3)
1.10	m_σ	0.26(3)	0.46(8)	0.99(4)	1.29(6)
1.20	m_π	0.06(2)	0.169(13)	0.31(2)	0.39(3)
1.20	m_σ	0.24(3)	0.40(7)	1.09(3)	1.28(6)

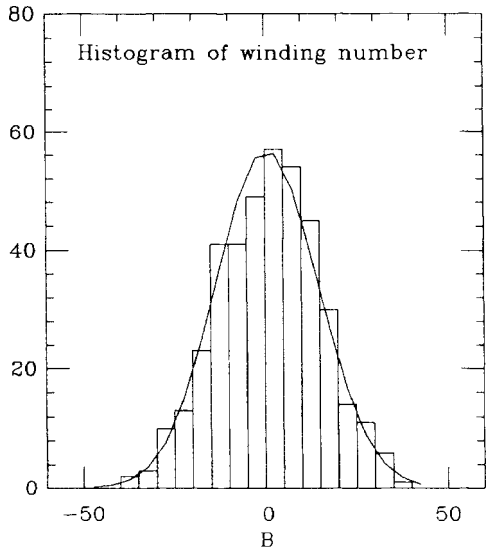

FIG. 7. Same as Fig. 6, but for a 20^3 lattice.

IV. SKYRME STABILIZATION

With a Skyrme term included, the continuum-O(4)-nonlinear chiral model in three dimensions has stable zero-temperature Skyrmion configurations. In an effort to enhance stability, we add the term

$$H_{\rm stab}/E = -\tfrac{1}{8}\beta_2 \sum_{(\mathbf{rstu})} \mathrm{Tr}\{U(\mathbf{t})^\dagger[U(\mathbf{t}) - U(\mathbf{r})], U(\mathbf{t})^\dagger[U(\mathbf{s}) - U(\mathbf{u})]\}^2, \quad (18)$$

which is a crude discrete version of a continuum Skyrme term, based on nearest-neighbor derivatives. Our discrete Skyrme action is similar to one proposed a few years ago by Saly.[8] However, we prefer to use the conventional sign for the Skyrme coupling. The sum over **(rstu)** refers to sites distributed around a unique plaquette, with the sites listed in cyclic order around the plaquette, i.e., **t** refers to the diagonal next neighbor to **r** and **s** is similarly related to **u**. After obvious algebraic simplification this particular lattice form of the Skyrme term was chosen for economy in the numerical algorithm. [Having $U(\mathbf{r})$ appear only once in this expression improves somewhat the efficiency of an otherwise rather time-consuming Metropolis update.]

The naive continuum limit of this term is then

$$H_{\rm stab} = -\frac{1}{32e^2}\int d\mathbf{r}\,\mathrm{Tr}[U^\dagger\partial_\mu U, U^\dagger\partial_\nu U]^2, \quad (19)$$

suggesting the identification

$$\beta_2 = 1/(8aE_0e^2). \quad (20)$$

Saly studied the phase structure of the $\beta_3 = 0$ version of a similar model in two and four dimensions as a function of β_1 and β_2 for negative values of β_2. His goal was to identify a nontrivial fixed point permitting a proper continuum limit of the theory. None was evident. However, the region $\beta_2 > 0$ remains to be explored. Since the limit $\beta_2 \to \infty$ corresponds to an infinitely large Skyrmion, it is quite possible that the desired fixed point is reached there. Our purpose here is to study finite-temperature symmetry restoration, treating the model, where necessary, as a discrete approximation to the continuum version, regardless of whether a nontrivial fixed point exists.

We find that with the Skyrme term present, and with our stochastic relaxation algorithm, large, classically stable Skyrmions can be constructed for $\beta_2 > 7$ at zero temperature, but not for smaller values of β_2. Because we are working on a three-dimensional lattice, these configurations correspond to classical solutions of the field equations. To produce such configurations, the lattice was initialized to a field configuration approximating closely the known continuum classical Skyrmion.[12] The configuration was then relaxed using the same Metropolis algorithm as in the thermal simulations, except that only small random steps were taken, and only steps reducing the energy were accepted. A stable local minimum of the energy was found. As expected from the known continuum configuration and the correspondence between lattice and continuum parameters, these large Skyrmions have rms radii in excess of $5a$. Similar discrete approximations to the continuum solution have been obtained by Jackson and Verbaarschott.[13] Thus, in principle, by making the lattices sufficiently large, we might hope to obtain the ideal model with nearly stable zero-temperature baryons. However, these large Skyrmions are not robust, since we were not able to produce them either by relaxing from a starting configuration with the correct topological properties, but a somewhat different radial wave function, or from rapidly cooled thermally excited configurations. Instead the configurations relaxed to the conventional symmetry-broken vacuum. Evidently, our lattice Hamiltonian does not assign a large enough penalty to configurations with sharp bends, making it too easy for a large Skyrmion to unwind.

Clearly to make further progress, one should explore other choices for the Hamiltonian. However, it turns out that there is another remedy available within the parameter space of the present Hamiltonian that brings us closer to our desired goal of a robust zero-temperature baryon: namely, at *negative* values of the lattice Skyrme coefficient β_2 there is a narrow range over which baryonic structures appear with an rms radius of approximately two lattice units and a lifetime of a few tens of lattice sweeps at low temperatures. With this choice of parameters, we obtain a model with reasonably persistent, small baryons at low temperature and chiral properties virtually the same as with the unstabilized model. For the moment, this small-Skyrmion model is the best we have to offer. Of course, with negative values of β_2, one cannot use Eq. (20).

It is in the nature of our discrete approximation to the lattice derivative that the kinetic energy of very

small Skyrmion configurations decreases as the Skyrmion shrinks. This behavior is contrary to what is found in the continuum limit, where the kinetic energy scales inversely with Skyrmion size. Thus, it should not be surprising that stability is improved by introducing a term in the Hamiltonian that discourages the development of a constant field configuration, and encourages a curvature that is typical of the Skyrme configuration. That is the reason a small negative value of β_2 works.

As Saly pointed out, in choosing negative β_2, one must avoid encountering a transition to an unphysical puckered phase. Shown in Fig. 8 is the value of $H_{\rm stab}$, averaged over the lattice volume, as a function of β_2. The starting configuration was the puckered lattice. While β_1 was fixed at a very low temperature ($\beta_1 = 50$), the value of β_2 was increased in two runs, one with a higher rate of increase than the other, and decreased in a third run. The third run was not carried to a full transition to the puckered phase. Evidently there is very strong hysteresis, indicating the presence of a strong first-order phase transition to the puckered phase at approximately $\beta_2 = -0.35$. We chose $\beta_2 = -0.30$, comfortably away from the phase transition.

To illustrate how the choice of β_2 affects Skyrmion stability, we show in Fig. 9 the total baryon number computed with the estimate (9) as a function of a Monte Carlo sweep at $\beta_1 = 50$, starting from a single-Skyrmion-like lattice configuration. This starting configuration filled the lattice with a spherically symmetric Skyrmion with a radial wave function that varied linearly with radius. The estimated baryon number was initially close to one, and then decreased as the Skyrmion relaxed to a smaller size. Since the smaller Skyrmions have larger curvature, the approximant (9) underestimates the true

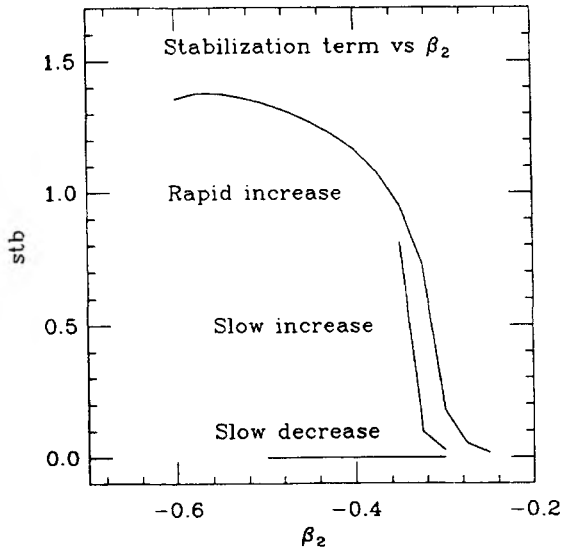

FIG. 8. Hysteresis at the phase transition to the puckered phase. Mean value of the stabilization energy as a function of the stabilization weight β_2 for three runs, two increasing β_2 and one decreasing β_2. In all runs $\beta_1 = 50$.

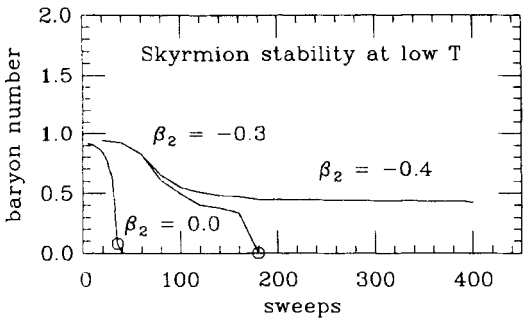

FIG. 9. Decay of a large Skyrmion configuration for various choices of the stabilization coefficient. The approximate baryon number is shown as a function of cooling sweep at $\beta_1 = 50$. The circle indicates the point at which the winding number changes from one to zero. At $\beta_2 = -0.4$ the winding number remains at one.

value. Also indicated in the plot is the point where the winding number switched from 1 to 0. We see that as β_2 increases in magnitude, the "lifetime" of the Skyrmion increases. Indeed for $\beta_2 = -0.4$ the small Skyrmion appears to be very stable, but at this parameter value the lattice is unstable against decay to the puckered phase. (Because of the metastability of the normal phase at this value of β_2 this run remained normal.) Also evident in these plots is that the approximate baryon number appears to reach a region of slow decay for a duration of about 50 sweeps at a baryon number of 0.4 before abruptly decaying. Of course, it is not possible to fix precisely the static properties of these classically unstable lumps. However, we believe an approximate determination can be made over the region of slow decay.

The spatial distribution of the Skyrmion can be visualized in a "snapshot" of baryon-number density versus lattice coordinate. Consider the configuration with $\beta_1 = -0.3$ at sweep 120 in Fig. 9. Shown in Fig. 10 is such a plot in flat perspective. A point is plotted for each lattice cube with approximate baryon-number density (9) greater than $0.003\,75/a^3$ in absolute value. Although it is not evident in this rendition, the central points have

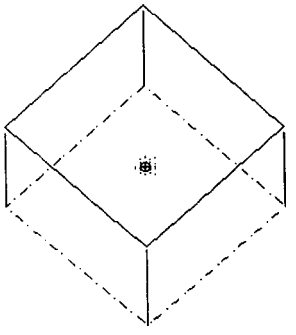

FIG. 10. A single small Skyrmion for $\beta_2 = -0.3$. Lattice in flat projection showing the location of points with approximate baryon density exceeding $0.003\,75/a^3$ in absolute value. Also indicated by a circle enclosing a plus sign is the point contributing +1 to the winding number.

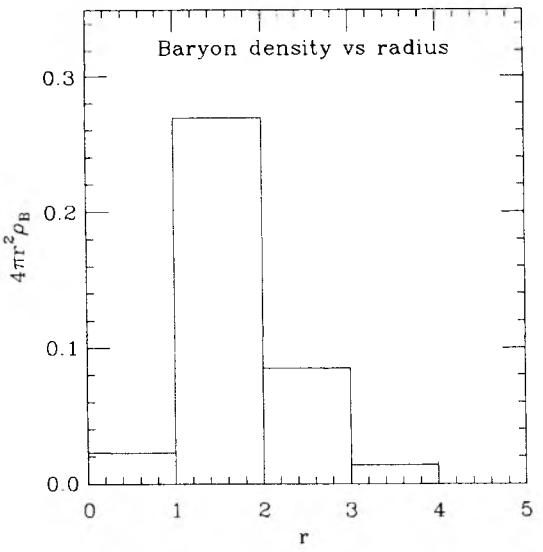

FIG. 11. Baryon density vs radius for the small Skyrmion of Fig. 10.

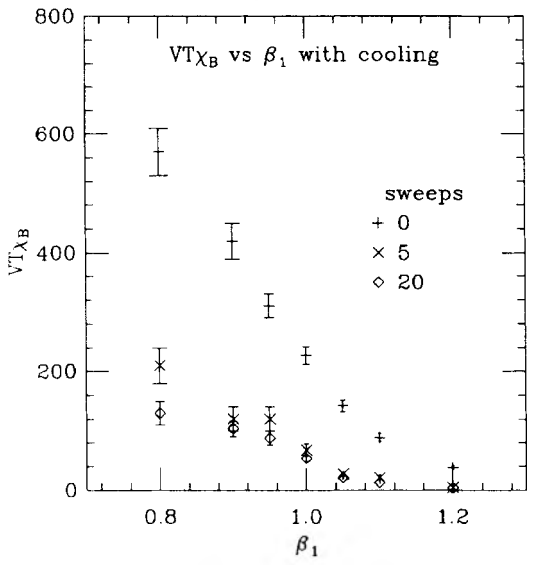

FIG. 13. Same as Fig. 5, but with $\beta_2 = -0.3$ and including measurements made after 5 and 10 cooling sweeps.

higher baryon number. Also indicated with a circled plus sign is the cell that contributes 1 to the winding number in Eq. (10). Shown in Fig. 11 is the baryon density for this configuration versus radius from the center of the distribution. We see that the baryon number density is indeed higher at the center. The rms size of this baryon is $1.9a$. The total energy of this structure is estimated to be $38E_0$ after subtracting a constant thermal background contribution. The radius and energy are both decreasing functions of sweep number as cooling progresses, and 40 sweeps later this structure relaxes abruptly to the symmetry-broken vacuum as indicated in Fig. 9. These configurations appear to be relatively robust in the sense that they are readily produced when cooling thermally excited configurations. These studies of Skyrmion-like configurations give us confidence that small negative values of β_2 have the desired effect of improving stability without evident adverse side effects.

Shown in Fig. 12 is the order parameter as a function of β_1 for $\beta_2 = -0.3$. Extrapolation to the chiral limit places the phase transition between 0.95 and 1.00. A plot of $\langle B^2 \rangle$ vs β_1 for the smallest values of β_3 is given in Fig. 13. Please refer for the moment to the points at zero cooling sweeps. Comparing with the $\beta_2 = 0$ calculation (Figs. 1 and 5), we see that in the present case the susceptibility is slightly lower and the phase transition occurs at a slightly lower temperature. Otherwise, the thermal behavior of the two models is quite similar.

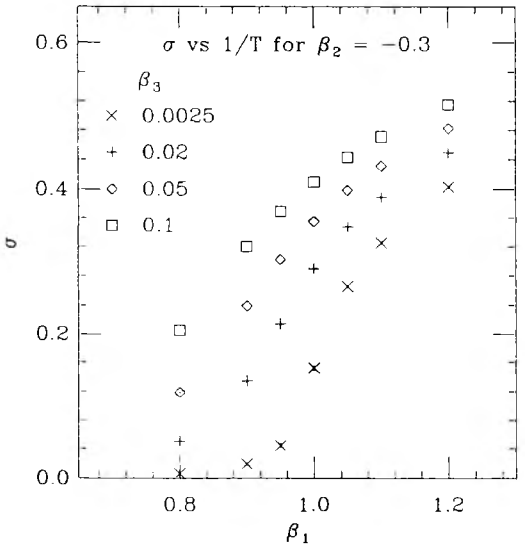

FIG. 12. Same as Fig. 1, but with $\beta_2 = -0.3$.

V. COOLED CONFIGURATIONS

In order to gain more insight into the mechanical features of symmetry restoration, a small sample of the lattices obtained in the simulation was subjected to rapid cooling, and a visual display of the resulting baryon density was made. The cooling process consisted of abruptly setting the inverse temperature β_1 to a large value, i.e., 50, and carrying out a few dozen Monte Carlo sweeps with Metropolis parameters set so that the acceptance rate was approximately 50%. This technique is intended to "smooth" out short-wavelength fluctuations with the hope of identifying long-wavelength structures.[14] The smoothing treatment is also suggestive of a dynamical process of rapid cooling, but no effort has been made here to develop a realistic simulation of a physical cooling process. Shown in Fig. 14 is a typical cooling sequence. Here the starting configuration is a representative of the thermal ensemble at $\beta_1 = 1.05$, a temperature near, but below the phase transition. As in Fig. 10 the plotted points in each frame represent cells in which the absolute value

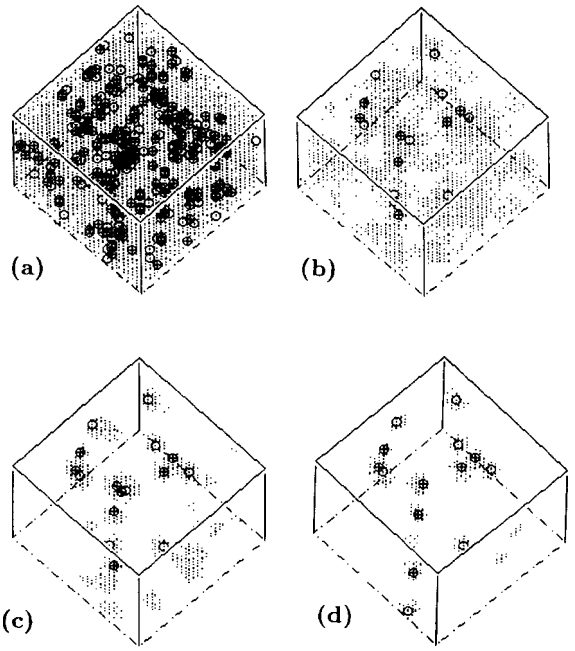

FIG. 14. Cooling sequence for a sample configuration thermalized just below the phase transition: (a) starting configuration, (b) after 10 sweeps, (c) after 20 sweeps, (d) after 50 sweeps. Points are plotted as in Fig. 10. Open circles represent points contributing -1 to the winding number.

of the estimated baryon density exceeds $0.00375/a^3$. We see that after a treatment of 20 sweeps, isolated structures resembling the Skyrmion of Fig. 10 become clearly identifiable, and some eventually decay.

To confirm that these structures resemble the Skyrmion, the baryon lumps in the configurations in the sample cooling sequence of Fig. 14 were studied individually to determine their baryon density, energy density, and rms size. The centroid of each lump was found by scanning for the center of the baryon distribution. The distribution in baryon number was measured out to a radius at which either the sign of the baryon density changed or the baryon density began to increase (usually because of a neighboring baryon). Almost all lumps had winding number ± 1. Occasionally a lump was found with winding number 2. Table II shows such an inventory at cooling sweep 10. The mean adjusted lump energy is $(30 \pm 3)E_0$ and the mean estimated baryon number is $(0.37 \pm 0.02)a$. All but one of these lumps survived 40 more cooling sweeps, after which the run was stopped.

Since the cooling process is stochastic, it is useful to repeat the cooling scenario with a different random-number seed to see whether the same pattern of lumps is recovered. It was not. Although the numbers of Skyrmions and anti-Skyrmions obtained was found to be similar, the lump distribution obtained was quite different. Thus the pattern of lumps is not attributable to the original configuration even if the rough multiplicity of lumps can be so ascribed.

From these and other visual studies, one may surmise that typical configurations close to the phase transition,

TABLE II. Inventory of Skyrmions from Fig. 14(b). Listed is the coordinate x, y, z of the center of the lump, the winding number B, the approximate total baryon number $b_{\rm tot}$, the background-subtracted total energy $E_{\rm adj}$, and the baryon-weighted rms radius $r_{\rm rms}$.

x, y, z	B	$b_{\rm tot}$	$E_{\rm adj}$	$r_{\rm rms}$
5, 24, 14	-1	-0.25	38	1.26
11, 22, 8	-1	-0.22	30	1.43
1, 14, 21	1	0.24	26	1.51
11, 24, 11	1	0.34	32	1.75
17, 6, 10	-1	-0.40	30	1.76
27, 8, 21	-1	-0.38	19	1.79
4, 15, 28	-1	-0.39	57	1.83
9, 24, 28	-1	-0.38	32	1.84
27, 26, 18	1	0.35	19	1.86
29, 18, 18	-1	-0.43	24	1.87
12, 30, 20	-1	-0.44	36	1.91
20, 3, 16	1	0.42	25	1.93
9, 29, 25	1	0.44	18	1.95
25, 20, 2	1	0.43	12	1.99
3, 20, 14	1	0.48	46	2.21

but in the symmetry-broken phase, do not have clearly distinguishable baryons. The typical "baryon density," i.e., curvature of the map (9) in the high-temperature configuration, is not very high, being only somewhat smaller in magnitude than the curvature within a single low-temperature Skyrmion. However, the sign of the baryon density fluctuates strongly, leading by random walk to the development of a nonzero winding number. Despite the apparent randomness of these fluctuations, the correlation length, determined from the pion screening mass, is quite large below the phase transition, falling sharply only above. A visual examination of the configurations during the cooling process reveals that regions

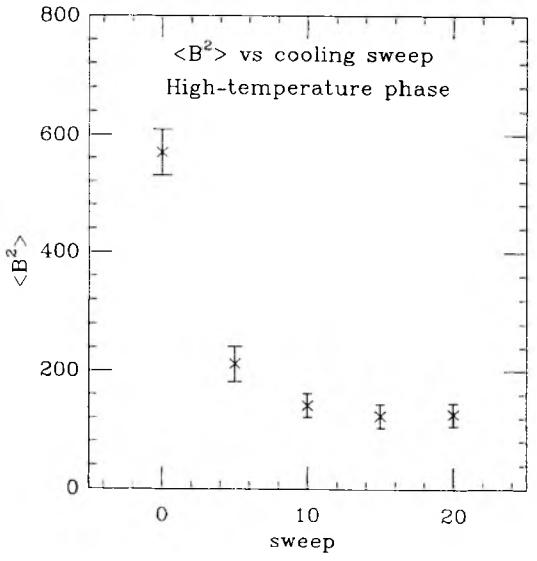

FIG. 15. Cooling history, showing the mean variance in baryon number, starting from configurations thermalized at $\beta_1 = 0.80$ (high-temperature phase).

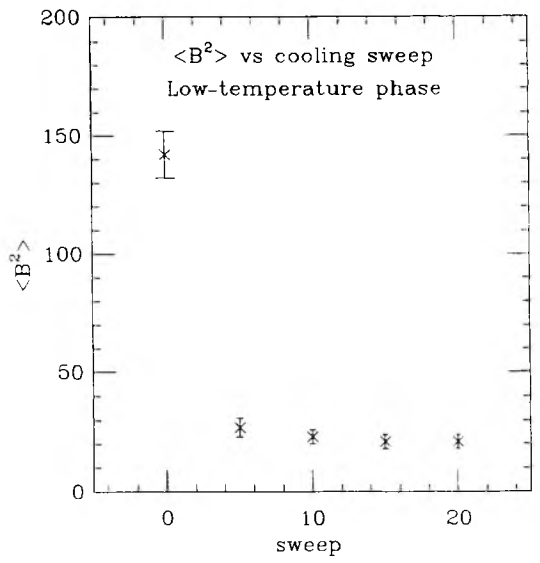

FIG. 16. Same as Fig. 15, but for $\beta_1 = 1.05$.

with a definite sign for the baryon density appear to gradually grow, then condense to small, isolated distinguishable Skyrmions. In the process of smoothing, the lattice cells contributing plus or minus one to the winding number are rapidly thinned out, leaving a residue in more-or-less one-to-one correspondence with the emerging Skyrmions.

To study the effect of cooling further, a large sample of configurations in an equilibrium thermal run was subjected to the same cooling treatment. The mean square of the winding number of this sample over the cooling history is plotted both above and below the phase transition in Figs. 15 and 16. It is evident that the value decays sharply in the first few sweeps, followed by a rather slow decay characteristic of the small Skyrmions. In Fig. 13 is shown the value obtained after 0, 5, and 10 cooling sweeps as a function of β_1. The relative stability of the "frozen" structures noted in the sample sequence after 10 cooling sweeps is evidently typical of the population.

VI. CONCLUSIONS AND DISCUSSION

We have shown that as the temperature increases past the chiral phase transition, the lattice chiral model shows an increase in topological susceptibility, as measured by the winding number. How realistic is this susceptibility? Because the lattice action we use permits strong curvature in the field configuration, one might argue that the topological susceptibility has been exaggerated over what would be expected from the continuum model. In somewhat similar studies of lattice gauge theories, it has been popular to take the residue of lumps in a given configuration that survive a cooling treatment as a more appropriate measure of the topological susceptibility.[14] With such an interpretation the curve for ten cooling sweeps in Fig. 13 would be supposed to be more representative of the susceptibility. Even this measure of the susceptibility shows a substantial rise as the temperature increases through the phase transition. To resolve these questions requires further study with more curvature-resistant lattice actions and, perhaps, also with the explicit introduction of fermions to give an independent measure of the fermion susceptibility.

For small values of the Skyrme-stabilization coefficient in our model, the low-temperature structures are relatively small configurations (2) with nonzero winding number. If we suppose that these structures are nucleons, we may estimate the physical size of the lattice and compare the measured susceptibility with that of full QCD. Comparing the known charge radius and mass of the nucleon with the observed parameters of these low-temperature structures, we should then estimate that $a \approx 0.4$ F and $E_0 \approx 30$ MeV. Since the phase transition occurs at a value of $\beta_1 \approx 1$, we must then conclude from (7) that the temperature of the phase transition in this model is approximately 30 MeV. Since QCD estimates of the temperature of the phase transition are typically four times higher or more, we conclude that this model cannot be compared reliably with QCD.

The lattice QCD value for the susceptibility just above the phase transition is approximately[1]

$$\chi_{B\mathrm{QCD}} \approx 0.22/a^2. \tag{21}$$

Setting the lattice scale from the temperature to $1/4a = 125$ MeV (Ref. 5) gives a value $\chi_{B\mathrm{QCD}} \approx 0.055$ GeV^2 just above the phase transition. The present chiral model gives

$$\chi_B = \langle B^2 \rangle / VT. \tag{22}$$

For the choice $\langle B^2 \rangle = 500$ and with the values $a \approx 0.4$ F and $T \approx 30$ MeV we obtain $\chi_B \approx 0.08$ GeV^2. However, in view of the unphysically small value of T in the model one might hope to claim only an order-of-magnitude agreement.

In view of the large Boltzmann suppression factor, how could baryons with their huge mass-to-temperature ratios possibly have any effect on the phase transition? (In the present example the mass-to-temperature ratio is approximately 30 at the phase transition.) The answer evidently lies in the large entropy associated with fluctuations in the baryon number. These excitations correspond to coherent fluctuations in the pion field. One might be tempted to associate them with highly excited baryons or isobars, but because in the present model configurations close to the phase transition do not reveal any readily identifiable isolated lumps, one must regard these configurations as a complicated ensemble of interacting mesonic and baryonic degrees of freedom.

This study supports suggestions made by several authors concerning a possible signal for quark-plasma formation.[15] In this "Kibble" mechanism, the chiral order parameter finds itself randomly oriented as the plasma cools, leading naturally to the formation of baryons and antibaryons. Because the susceptibility is found to be

numerically rather large, it is expected that antiproton production in heavy-ion collisions resulting in plasma formation would be copious, perhaps more than is expected from simple high-energy pair production or through random recombination from antiquarks.[16] Calculations with models inspired by these lattice studies are needed to estimate how many antibaryons survive final-state annihilation.

It should be emphasized that the mechanism of chiral-symmetry restoration proposed here permits a natural connection between high-temperature and high-density symmetry restoration. At high baryon number density, chiral symmetry should be restored as a result of the chaotic rearrangement of the order parameter, brought about by the proliferation of baryons (with little or no antibaryonic involvement). Thus one should expect a continuous phase boundary connecting these two regimes. Classical studies of high-density symmetry restoration have been carried out on a "crystalline" field configuration by Jackson and Verbaarschott.[13] In the context of the lattice model there seem to be no serious technical obstacles to including a baryonic chemical potential in the action and exploring the complete phase boundary.

ACKNOWLEDGMENTS

I thank Osamu Miyamura for discussions that stimulated my interest in this problem and Yong-shi Wu and Al Mueller for helpful suggestions. This work was supported in part by the National Science Foundation under Grant No. NSF-PHY8706501. Computations were carried out on a Cray X-MP/48 at the San Diego Supercomputer Center and on an IBM 3090/600S at the Utah Supercomputer Institute. I thank both supercomputer centers for generous support. Help from the University of Utah Research Committee is also gratefully appreciated. It is a pleasure to acknowledge the hospitality of the Research Institute for Fundamental Physics at Kyoto University, where this work began.

[1] S. Gottlieb, W. Liu, D. Toussaint, R. Renkin, and R. Sugar, Phys. Rev. Lett. **59**, 2247 (1987).

[2] C. E. DeTar and J. B. Kogut, Phys. Rev. D **36**, 2828 (1987); Phys. Rev. Lett. **59**, 399 (1987); S. Gottlieb, W. Liu, D. Toussaint, R. L. Renkin, and R. L. Sugar, *ibid.* **59**, 1881 (1987); A. Gocksch, P. Rossi, and U. Heller, Phys. Lett. B **205**, 334 (1988).

[3] L. Dolan and R. Jackiw, Phys. Rev. D **9**, 3320 (1974); S. Weinberg, *ibid.* **9**, 3357 (1974).

[4] J. B. Kogut and D. K. Sinclair, Nucl. Phys. **B280**, 625 (1987), and references therein.

[5] S. Gottlieb, W. Liu, D. Toussaint, R. L. Renkin, and R. L. Sugar, Phys. Rev. Lett. **59**, 1513 (1987).

[6] H. Goldberg, Phys. Lett. **131B**, 133 (1983).

[7] T. H. R. Skyrme, Nucl. Phys. **31**, 556 (1962).

[8] R. Saly, Phys. Rev. D **31**, 2652 (1985).

[9] E. Witten, Nucl. Phys. **B223**, 433 (1983).

[10] J. Goldstone and R. L. Jaffe, Phys. Rev. Lett. **51**, 1518 (1983); S. Kahana and G. Ripka, Nucl. Phys. **A429**, 462 (1984).

[11] J. Kogut, M. Snow, and M. Stone, Nucl. Phys. **B200**, 211 (1981); J. Kogut, M. Stone, H. W. Wyld, S. H. Shenker, J. Shigemitsu, and D. K. Sinclair, *ibid.* **B225**, 326 (1983).

[12] G. Adkins, C. Nappi, and E. Witten, Nucl. Phys. **B228**, 552 (1983).

[13] A. D. Jackson and J. J. M. Verbaarschott, Nucl. Phys. **A494**, 419 (1988).

[14] M. Teper, Phys. Lett. **162B**, 357 (1985); Phys. Lett. B **171**, 81 (1986); **171**, 86 (1986).

[15] T. W. B. Kibble, J. Phys. A **9**, 1387 (1976); T. A. DeGrand, Phys. Rev. D **30**, 2001 (1984); J. Ellis and H. Kowalski, Phys. Lett. B **214**, 161 (1988); Nucl. Phys. **B327**, 32 (1989); A.H. Mueller, in *Quark Matter '88*, proceedings of the Seventh International Conference on Ultrarelativistic Nucleus-Nucleus Collisions, Lenox, Massachusetts, 1988, edited by G. Baym, P. Braun-Munzinger, and S. Nagamiya [Nucl. Phys. **A498** (1989)].

[16] U. Heinz, P. R. Subramanian, and W. Greiner, Z. Phys. A **318**, 247 (1984); J. Phys. G **12**, 1237 (1986); P. Koch, B. Müller, H. Stöcker, and W. Greiner, Mod. Phys. Lett. A **3**, 737 (1988).